VOLUME 111, NUMBER 24
NOVEMBER 22, 1989
© *Copyright 1989 by the American Chemical Society*

JOURNAL
OF THE
AMERICAN
CHEMICAL
SOCIETY

Unusual Structural Distortions Induced by Charge-Transfer Interactions through Conjugated Molecules: Crystal Structures of $NH_2C_6H_4(C{\equiv}C)_nC_6H_4NO_2$ (n = 0–3)

Eva M. Graham,[†] Vincent M. Miskowski,[†] Joseph W. Perry,[†] Daniel R. Coulter,[†] A. E. Stiegman,[*,†] William P. Schaefer,[*,‡] and Richard E. Marsh[*,‡]

Contribution from the Jet Propulsion Laboratory, California Institute of Technology, Pasadena, California 91109, and the Arthur Amos Noyes Laboratory of Chemical Physics, Division of Chemistry and Chemical Engineering, California Institute of Technology, Pasadena, California 91125. *Received January 6, 1989*

Abstract: A detailed structural analysis of the series of donor–acceptor molecules $O_2NC_6H_4(C{\equiv}C)_nC_6H_4NH_2$ (n = 0–3) has been performed in order to investigate ground-state donor–acceptor interactions through a conjugated framework. The results of the investigation reveal an unusual bonding pattern that is not adequately explained by a simple quinonoid resonance structure resulting from bond migration through the conjugated backbone. Instead, the charge-transfer character manifests itself through quinonoid distortions *only* of the nitrophenyl and aminophenyl functional groups themselves. Evidence is presented that indicates an intramolecular origin for the charge transfer. The acetylene bridges, which *must* participate in the migration of charge, are not themselves structurally altered. These observations lead to the conclusion that the charge-transfer character in the ground state is not highly delocalized but results in charges localized in the acceptor orbitals. Weak powder second harmonic generation was observed from the compounds with n = 1–3. This is discussed relative to the single-crystal X-ray structures.

Molecules containing both electron donor and acceptor functional groups that communicate strongly through a conjugated molecular framework display a variety of unusual structural and electronic properties. From a structural standpoint, the existence of donor and acceptor groups in the same molecule results in a redistribution of charge, from donor to acceptor, leading to substantial distortions of the molecular framework.[1] These same donor–acceptor interactions profoundly affect the electronic structure of the molecule, resulting in unusual spectroscopic and photophysics properties. *Intra*molecular charge-transfer transitions (ICT), in which optical excitation leads to a movement of charge from the donor group to the acceptor group, is a characteristic feature of this type of molecule.[2] Implicit in charge-transfer transitions is the sudden redistribution of charge in the excited state, which yields large excited-state dipole moments.[3] It is this sudden creation of large dipole moments that produces many of the interesting linear and nonlinear spectroscopic effects. Extensive work by Rettig, Lippert, and others[4] has shown that many organic donor–acceptor molecules, such as (dimethylamino)benzonitrile, undergo profound structural changes in the excited state. This creation of a "twisted" excited state can manifest itself spectroscopically by the presence of two emissions, one emanating from

---

[†] Jet Propulsion Laboratory.

[‡] Arthur Amos Noyes Laboratory of Chemical Physics.

(1) (a) Colapietro, M.; Domenicano, A.; Marciante, C.; Portalone, G. *Z. Naturforsch.* **1982**, *37B*, 1309–1311. (b) Mak, T. C. W.; Trotter, J. *Acta. Crystallogr.* **1965**, *18*, 68–74.

(2) Jaffe', H. H.; Orchin, M. *Theory and Application of Ultraviolet Spectroscopy*; John Wiley and Sons: New York, 1962; pp 259–264.

(3) (a) Lakowicz, J. R. *Principles of Fluorescence Spectroscopy*; Plenum Press: New York, 1983. (b) Mataga, N.; Kubota, T. *Molecular Interactions and Electronic Spectra*; Marcel Dekker: New York, 1970.

(4) (a) Rettig, W. *Angew. Chem., Int. Ed. Engl.* **1986**, *25*, 971–988. (b) Lippert, E.; Rettig, W.; Bonacic'-Koutecky', V.; Heisel, F.; Meihe, J. A. *Adv. Chem. Phys.* **1987**, *68*, 1–173. (c) Bonacic-Koutecky, V.; Koutecky, J.; Michl, J. *Angew. Chem., Int. Ed. Engl.* **1987**, *26*, 170–189.

0002-7863/89/1511-8771$01.50/0 © 1989 American Chemical Society

Table I. Crystal Data, $O_2NC_6H_4(C{\equiv}C)_nC_6H_4NH_2$

	compound			
	I (n = 0)	II (n = 1)	III (n = 2)	IV (n = 3)
formula	$C_{12}H_{10}N_2O_2$	$C_{14}H_{10}N_2O_2$	$C_{16}H_{10}N_2O_2$	$C_{18}H_{10}N_2O_2$
fw	214.23	238.25	262.27	286.29
cryst system	orthorhombic	orthorhombic	monoclinic	monoclinic
space group	$Pca2_1$	$Pbcn$	$P2_1/c$	$P2_1/c$
a, Å	24.407 (5)	14.447 (2)	8.412 (2)	8.426 (1)
b, Å	5.818 (1)	5.910 (1)	6.047 (1)	6.003 (3)
c, Å	7.417 (2)	27.802 (3)	25.083 (5)	28.835 (4)
β, deg	(90)	(90)	89.68 (2)[a]	96.76 (1)
V, Å^3	1053.2	2373.8	1264.9	1448.4
Z	4	8	4	4
d_{calcd}, g·cm^{-3}	1.351	1.333	1.365	1.313
λ, Å	0.71073	0.71073	0.71073	0.71073
crystal size, mm	0.12 × 0.15 × 0.16	0.34 × 0.33 × 0.16	0.07 × 0.19 × 0.44	0.6 × 0.22 × 0.4
μ, cm^{-1}	1.0	1.0	1.0	1.0
2θ range, deg	2–50	2–50	2–50	2–50
scan speed, deg/min	2	2	2	2
scan type	ω	ω	θ–2θ	ω
octants collected	$\pm h,k,l$	$h,\pm k,l$	$\pm h,\pm k,l$	$\pm h,\pm k,l$
no. of unique reflcns measd	2247	4542	4671	5276
no. of indep reflcns	1003	2078	2239	2539
GOF, for merging	0.97	0.97	0.94	1.03
no. with $F^2 > 0$	826	1655	1707	2278
no. with $F^2 > 3\sigma(F^2)$	506	1068	1015	1551
final R, $F^2 > 0$	0.066	0.070	0.076	0.056
final R, $F^2 > 3\sigma(F^2)$	0.034	0.041	0.040	0.036
final GOF,[b] all data	1.34	1.65	1.49	1.71

[a] β is taken as acute to emphasize the structural similarity between compounds III and IV. [b] GOF = $[\sum W(F_o^2 - F_c^2)^2/(n-p)]^{1/2}$.

the planar and the other from the twisted excited state. Another characteristic of the highly polar excited state is the pronounced solvatochromism of absorption and emission bands shown by many donor–acceptor molecules.[3] In addition, donor–acceptor molecules have come under intense study because of their nonlinear optical properties. Conjugated molecules possessing strong ICT transitions show large second-order molecular hyperpolarizabilities, which, in a suitable solid-state environment (noncentrosymmetric space group), can result in second harmonic generation (SHG).[5]

In an effort to investigate the properties of conjugated donor–acceptor molecules in a systematic fashion we have synthesized a series of compounds of the general structure

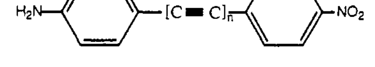

I, II, III, IV: n= 0, 1, 2, 3

where the number of acetylene links is varied from 0 to 3. Previously we reported solution spectroscopic results for this series in which we observed that increasing the conjugated donor–acceptor distance has little effect on the energy and intensity of the ICT band.[6] We report here the results of crystal structure analyses of this series of molecules. A number of interesting features of the bonding and charge distribution for this class of molecules emerge from the structure determinations.

Experimental Section

Pyridine (Baker) was dried over calcium hydride and distilled before use. All other solvents were reagent grade and used as received. Freshly precipitated cuprous chloride was used in making the Hay catalyst.[7] The p-iodoaniline (Aldrich) was used without further purification. (Nitrophenyl)acetylene,[8] (aminophenyl)acetylene,[8] and (triethylsilyl)acetylene[7b] were synthesized by literature methods. Infrared spectra were acquired as solid-state diffuse reflectance spectra on an Analect 6160 FTIR spectrophotometer.

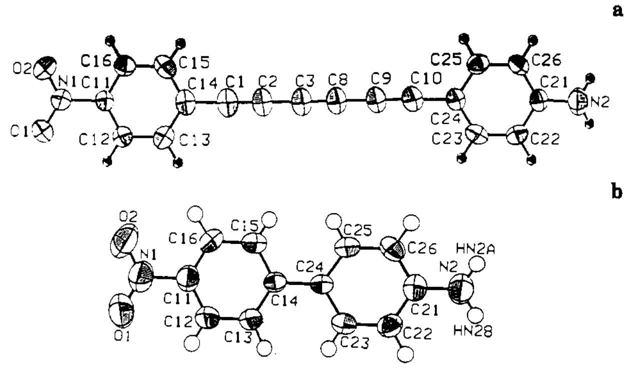

Figure 1. ORTEP labeling diagram of (a) IV and (b) I. The thermal ellipsoids are shown at 50% probability level; hydrogen atoms were given arbitrary small radii.

Crystallographic structure calculations were done with programs of the CRYM crystallographic computing system, MULTAN and ORTEP. Scattering factors and corrections for anomalous scattering were taken from a standard reference.[9] The parameters used to evaluate the quality of the structure are $R = \sum|F_o - |F_c||/\sum F_o$ for only $F_o^2 > 0$, and goodness of fit = $[\sum w(F_o^2 - F_c^2)^2/(n-p)]^{1/2}$ where n is the total number of reflections and p the number of parameters refined. The function minimized in least squares was $\sum w(F_o^2 - F_c^2)^2$, where $w = 1/\sigma^2(F_o^2)$. Variances of the individual reflections were assigned based on counting statistics plus an additional term, $0.014I^2$. Variances of the merged reflections were determined by standard propagation of error plus an additional term, $0.014\langle I\rangle^2$. For all of the structures small crystals were selected, glued with epoxy to a glass fiber, and centered on a diffractometer. Unit cell dimensions and the orientation matrix were obtained from the setting angles of 25 reflections with 16° < 2θ < 25°; an average background as a function of 2θ was calculated and applied to all reflections; Lp factors were also applied. No absorption corrections were made because the absorption coefficients and the crystals were small. Details of the X-ray diffraction studies are summarized in Table I. Atom coordinates are given in Table II; anisotropic coefficients U_{ij} and tables of F_o and F_c are available as supplementary material. The atom numbering scheme is shown in Figure 1; this scheme is general for all of the

---

(5) Chemla, D. S.; Zyss, J. In *Nonlinear Optical Properties of Organic Molecules and Crystals*; Chemla, D. S., Zyss, J., Eds.; Academic Press: New York 1987; Vol. I, p 23.

(6) Stiegman, A. E.; Miskowski, V. M.; Perry, J. W.; Coulter, D. R. *J. Am. Chem. Soc.* **1987**, *109*, 5884–5886.

(7) (a) Hay, A. S. *J. Org. Chem.* **1962**, *27*, 3320–3321. (b) Eastmond, R.; Johnons, T. R.; Wlaton, D. R. M. *Tetrahedron* **1972**, *28*, 4601–4616.

(8) (a) Wentworth, S. E.; Libby, J. B.; Berquist, P. R. report AMMRC-TR-84-23; order AD-14460, available from NTIS, 1984. (b) Takahashi, S.; Kuroyama, K.; Sonogashira, N.; Hagihara, H. *Synthesis* **1980**, 627–630.

(9) *International Tables for X-ray Crystallography*; Kynoch Press: Birmingham, U.K., 1974; Vol. IV, p 71, 149.

Table II. Fractional Coordinates and Equivalent Isotropic Temperature Factors (Å^2) for Compounds I–IV

	X ($\times 10^4$)	Y ($\times 10^4$)	Z ($\times 10^4$)	U_{eq} ($\times 10^4$)^a		X ($\times 10^4$)	Y ($\times 10^4$)	Z ($\times 10^4$)	U_{eq} ($\times 10^4$)^a
				Compound I (n = 0)					
N(1)	7619 (2)	5254 (9)	8414 (12)	854 (19)	C(16)	8334 (2)	2620 (11)	9471 (11)	760 (20)
O(1)	7514 (2)	7054 (8)	7624 (13)	1187 (16)	N(2)	11514 (2)	350 (10)	8911 (13)	809 (18)
O(2)	7274 (2)	3978 (8)	9088 (12)	1144 (18)	C(21)	10981 (2)	1080 (10)	8884	578 (15)
C(11)	8200 (2)	4596 (10)	8597 (11)	638 (17)	C(22)	10837 (2)	3188 (9)	8150 (13)	577 (16)
C(12)	8591 (2)	5994 (11)	7844 (13)	686 (18)	C(23)	10294 (2)	3910 (9)	8142 (13)	541 (16)
C(13)	9136 (2)	5333 (10)	7966 (12)	602 (16)	C(24)	9872 (2)	2586 (8)	8870 (11)	427 (12)
C(14)	9290 (2)	3313 (8)	8810 (11)	459 (13)	C(25)	10033 (2)	507 (9)	9637 (13)	540 (16)
C(15)	8875 (2)	1996 (11)	9580 (14)	687 (18)	C(26)	10567 (2)	−236 (9)	9642 (13)	547 (16)
	X ($\times 10^4$)	Y ($\times 10^4$)	Z ($\times 10^5$)	U_{eq} ($\times 10^4$)^a		X ($\times 10^4$)	Y ($\times 10^4$)	Z ($\times 10^5$)	U_{eq} ($\times 10^4$)^a
				Compound II (n = 1)					
O(1)	1738 (2)	956 (4)	3235 (7)	922 (7)	C(1)	1216 (2)	7035 (4)	21684 (9)	512 (7)
O(2)	1030 (2)	3763 (3)	24 (7)	917 (7)	C(10)	1259 (2)	7947 (4)	25466 (10)	516 (7)
N(1)	1358 (2)	2804 (4)	3503 (8)	605 (7)	N(2)	1129 (2)	11751 (6)	43975 (10)	814 (9)
C(11)	1291 (2)	3888 (4)	8216 (8)	425 (6)	C(21)	1189 (2)	10860 (4)	39401 (9)	483 (6)
C(12)	1651 (2)	2774 (4)	1214 (9)	450 (6)	C(22)	1584 (2)	8744 (5)	38647 (10)	519 (7)
C(13)	1608 (2)	3793 (4)	16585 (9)	471 (7)	C(23)	1618 (2)	7831 (4)	34121 (10)	483 (10)
C(14)	1212 (2)	5940 (4)	17079 (8)	454 (6)	C(24)	1254 (2)	8975 (4)	30149 (8)	447 (6)
C(15)	838 (2)	7000 (5)	13026 (9)	492 (7)	C(25)	878 (2)	11117 (4)	30928 (9)	482 (7)
C(16)	878 (2)	5983 (4)	8575 (9)	476 (7)	C(26)	847 (2)	12039 (5)	35453 (9)	488 (7)
	X ($\times 10^4$)	Y ($\times 10^4$)	Z ($\times 10^5$)	U_{eq} ($\times 10^4$)^a		X ($\times 10^4$)	Y ($\times 10^4$)	Z ($\times 10^5$)	U_{eq} ($\times 10^4$)^a
				Compound III (n = 2)					
O(1)	212 (3)	−4179 (4)	14401 (9)	728 (7)	C(2)	3432 (4)	4215 (6)	−4912 (13)	573 (9)
O(2)	−1274 (3)	−1412 (4)	16435 (9)	784 (8)	C(9)	4162 (4)	5636 (6)	−8517 (14)	578 (9)
N(1)	−206 (3)	−2259 (4)	13769 (11)	507 (7)	C(10)	4813 (4)	6864 (5)	−11606 (13)	543 (9)
C(11)	590 (4)	−933 (5)	9689 (11)	397 (8)	N(2)	7985 (5)	12081 (7)	−26784 (15)	765 (11)
C(12)	1932 (4)	−1716 (5)	7219 (13)	461 (9)	C(21)	7172 (4)	10821 (6)	−23056 (12)	493 (9)
C(13)	2664 (4)	−453 (5)	3398 (13)	519 (9)	C(22)	7714 (4)	8728 (6)	−21788 (13)	509 (10)
C(14)	2057 (4)	1629 (5)	2105 (12)	475 (9)	C(23)	6951 (4)	7454 (6)	−18059 (14)	501 (9)
C(15)	694 (4)	2362 (6)	4638 (14)	522 (10)	C(24)	5614 (4)	8219 (5)	−15393 (12)	439 (8)
C(16)	−48 (4)	1113 (5)	8463 (13)	475 (9)	C(25)	5069 (4)	10350 (5)	−16619 (13)	494 (9)
C(1)	2818 (4)	3008 (5)	−1814 (13)	555 (9)	C(26)	5838 (4)	11602 (6)	−20411 (14)	520 (10)
	X ($\times 10^4$)	Y ($\times 10^4$)	Z ($\times 10^5$)	U_{eq} ($\times 10^4$)^a		X ($\times 10^4$)	Y ($\times 10^4$)	Z ($\times 10^5$)	U_{eq} ($\times 10^4$)^a
				Compound IV (n = 3)					
O(1)	−124 (2)	−4967 (2)	15513 (4)	784 (3)	C(3)	3448 (2)	4404 (3)	−4707 (6)	725 (5
O(2)	−1596 (1)	−2156 (2)	16751 (4)	847 (4)	C(8)	4020 (2)	5558 (3)	−7518 (6)	723 (5)
N(1)	−572 (2)	−3046 (2)	14728 (4)	577 (4)	C(9)	4679 (2)	6852 (3)	−10693 (6)	696 (5)
C(11)	152 (2)	−1765 (2)	11190 (5)	490 (4)	C(10)	5262 (2)	7986 (3)	−13487 (6)	647 (5)
C(12)	1442 (2)	−2631 (3)	9304 (6)	567 (4)	N(2)	7994 (2)	12937 (4)	−27002 (6)	814 (5)
C(13)	2116 (2)	−1392 (3)	6020 (6)	638 (5)	C(21)	7306 (2)	11734 (3)	−23679 (5)	538 (4)
C(14)	1497 (2)	695 (3)	4616 (5)	598 (5)	C(22)	7870 (2)	9608 (3)	−22408 (6)	580 (5)
C(15)	183 (2)	1496 (3)	6578 (6)	651 (5)	C(23)	7202 (2)	8425 (3)	−19088 (6)	581 (5)
C(16)	−496 (2)	291 (3)	9880 (6)	598 (5)	C(24)	5962 (2)	9279 (3)	−16858 (5)	534 (4)
C(1)	2212 (2)	2002 (3)	1277 (6)	720 (5)	C(25)	5416 (2)	11438 (3)	−18088 (5)	553 (4)
C(2)	2791 (2)	3121 (3)	−1505 (6)	715 (5)	C(26)	6072 (2)	12616 (3)	−21449 (6)	551 (4)

^{a} $U_{eq} = {}^1/_3\sum_i\sum_j[U_{ij}(a_ia_j)(\mathbf{a}_i{\cdot}\mathbf{a}_j)]$.

molecules with the addition or deletion of the central bridging carbon atoms.

***p*-Nitro-*p*′-aminobiphenyl.** Synthesis of *p*-nitro-*p*′-aminobiphenyl was by literature methods.[10] Orange-red X-ray quality crystals were obtained by slow cooling of a hot saturated CH_2Cl_2 solution. Two equivalent sets of data were obtained and merged; systematic absences in the diffractometer data were consistent with space groups *Pbcm* or (in a different setting) *Pca*2$_1$. The three check reflections showed no systematic variations. An initial try in space group *Pbcm* gave an image of the structure, but with a nonphysical geometry (nonplanar benzene rings). The correct solution appeared in *Pca*2$_1$ and the parameters were refined by full-matrix least squares. The final matrix included positional parameters for all atoms (*z* of C21 was held fixed), anisotropic thermal parameters for the non-hydrogen atoms, isotropic thermal parameters for the hydrogen atoms, a scale factor, and a secondary extinction parameter (final value, 0.95 (16 × 10^{-6})).[11] The final *R* index for the reflections with $F_o^2 > 3\sigma(F_o^2)$ was 0.034; the final difference map showed maximum excursions of ±0.24 e Å^{-3}.

***p*-Amino-*p*′-nitrodiphenylacetylene. a. Synthesis.** Cuprous (nitrophenyl)acetylene, $Cu(C{\equiv}CC_6H_4NO_2)$, was prepared by the method of Hooper.[12] In 150 mL of degassed pyridine were refluxed cuprous(nitrophenyl)acetylene (2.37 g) and *p*-iodoaniline (2.72 g) under inert atmosphere for 12 h. The pyridine was removed and the residue dissolved in methanol and filtered to remove CuI produced in the reaction. Removal of the methanol left on oily red residue, which solidified upon trituration with hexane. The solid was chromatographed on silica gel with methylene chloride/toluene (4/1) as elutant. The second dark orange band contained the desired product (1.42 g, 53% yield; mp 190 °C), which was recrystallized from a 1/1 mixture of CH_2Cl_2/hexane by slow evaporation: IR cm^{-1} 3489, 3389 (NH); 2208 (C≡C); 1510, 1337 (NO_2); ^{1}H NMR (500 MHz, $CDCl_3$) δ 3.93 (s, 2 H), 7.27 (m, 8 H). Anal. Calcd for $C_{14}H_{10}N_2O_2$: C, 70.58; H, 4.23; N, 11.76. Found: C, 70.47; H, 4.30; N, 11.73.

b. Crystallography. Dark red crystals were obtained by slow evaporation of an acetonitrile solution. Two equivalent sets of data were collected and merged; systematic absences in the diffractometer data uniquely determined the space group as *Pbcn*. The data were corrected for a slight decay. Five reflections with highly asymmetric backgrounds were deleted to give the final data set. The structure was refined by full-matrix least squares. After the heavy atoms had converged, hydrogen atoms were introduced at calculated positions; their coordinates and isotropic temperature factors were refined in the same matrix as the coordinates and anisotropic thermal parameters of the O, N, and C atoms, plus a scale factor and secondary extinction coefficient parameter (204 parameters). The secondary extinction parameter[11] was refined to 0.18 (3) × 10^{-6}. The final *R* index for reflections with $F_o^2 > 3\sigma(F_o^2)$ is 0.041. The final difference map showed maximum excursions of +0.39 and −0.24 e Å^{-3}, with no discernable pattern.

***p*-Amino-*p*′-nitrodiphenylbutadiyne. a. Synthesis.** (*p*-Nitrophenyl)acetylene (1.0 g) and (*p*-aminophenyl)acetylene (0.8 g) were coupled

---

[10] Idoux, J. P. *J. Chem. Soc. C* **1970**, 435–437.

[11] Larson, A. C. *Acta Crystallogr.* **1967**, *23*, 644, eq 3.

[12] Bond, C. C.; Hooper, M. *J. Chem. Soc. C* **1969**, 2453–2460.

overnight in acetone (50 mL) by using the Hay catalyst.[7] Water was added to the reaction mixture, and the organic product was extracted into ether. The ether solution was dried with sodium sulfate and evaporated, leaving a dark red solid. The crude compound was chromatographed on silica gel and eluted with 5/1 CH_2Cl_2/toluene. Two yellow bands eluted first, followed by a dark red band that contained 0.66 g (36% yield; mp 256 °C) of the desired product. Slow evaporation of the solvent mixture gave thin red crystals: IR cm^{-1} 3477, 3382 (NH_2); 2196 ($C{\equiv}C$); 1512, 1342 (NO_2); ^1H NMR (500 MHz, $CDCl_3$) δ 3.97 (s, 2 H), 7.27 (m, 8 H). Anal. Calcd for $C_{16}H_{10}N_2$: C, 73.28; H, 3.84; N, 10.68. Found: C, 72.68; H, 3.66; N, 10.57.

b. Crystallography. X-ray quality crystals were obtained from slow evaporation of an acetonitrile solution. Lorentz and polarization factors were applied and the equivalent data were merged to give the final data set. The structure was refined by full-matrix least squares; the final refinement included coordinates of all atoms, anisotropic thermal parameters for non-hydrogen atoms, isotropic thermal parameters for hydrogen atoms, a scale factor, and the secondary extinction parameters (222 parameters). The secondary extinction parameter[11] was refined to 0.15 (8×10^{-6}). The final R index for reflections with $F_o^2 > 3\sigma(F_o^2)$ is 0.040. The final difference map showed maximum excursions of +0.38 and −0.32 e Å^{-3} in no discernable pattern.

(*p*-Nitrophenyl)butadiyne. Synthesis. (*p*-Nitrophenyl)acetylene (1.0 g) and (triethylsilyl)acetylene (4.8 g) were coupled overnight in acetone (30 mL) by using the Hay catalyst.[7] The reaction mixture was diluted with water (150 mL) and extracted with petroleum ether (400 mL). The organic layer was separated, dried with magnesium sulfate, and evaporated, leaving an oily yellow residue. The yellow residue was chromatographed on alumina (neutral, activity 1) and eluted with ethyl ether/petroleum ether (1/4). The elutant was monitored by UV-Vis spectroscopy until it contained the silane protected product, $O_2NC_6H_4(C{\equiv}C)_2Si(C_2H_5)_2$.[13] Collection of this fraction and removal of the solvent yielded a pale yellow solid, which was subsequently dissolved in methanol (150 mL) and treated with 0.1N NaOH (50 mL). The solution was stirred for 3 h and neutralized with HCl, and the solvent was removed under vacuum. The residue was extracted into petroleum ether, dried with sodium sulfate, and allowed to evaporate yielding (.45 g, 38% yield based on (nitrophenyl)acetylene) (*p*-nitrophenyl)butadiyne.[14]

***p*-Amino-*p*′-nitrodiphenylhexatriyne. a. Synthesis.** (*p*-Nitrophenyl)butadiyne (0.2 g) and (*p*-aminophenyl)acetylene (0.28 g) were coupled overnight in acetone (30 mL) by using the Hay catalyst.[7] Water was added to the solution and the product was extracted with ether (1000 mL), dried with magnesium sulfate, and evaporated. The resulting red solid was chromatographed on silica gel with CH_2Cl_2/toluene (1/1). The second orange band isolated contained *p*-amino-*p*′-nitrodiphenylhexatriyne (0.11 g, 40% yield relative to (*p*-nitrophenyl)butadiyne): mp >240 °C dec; IR cm^{-1} 3505, 3410 (NH_2); 2160 ($C{\equiv}C$); 1507, 1342 (NO_2); ^1H NMR (500 MHz, $CDCl_3$) δ 4.00 (s, 2 H), 7.27 (m, 8 H). Anal. Calcd for $C_{18}H_{10}N_2O_2$: C, 75.52; H, 3.52; N, 9.79. Found: C. 75.01; H, 3.41; N, 9.80.

b. Crystallography. Slow evaporation of an acetonitrile solution produced dark red X-ray quality crystals. Two complete data sets out to $2\theta = 50°$ were collected and corrected for a small decay; the data were merged to give the final data set. No reflections were discarded. The structure was solved by MULTAN and refined by full-matrix least squares; the final matrix included positional parameters for all hydrogen atoms, anisotropic thermal parameters for non-hydrogen atoms (hydrogen isotropic), a scale factor, and a secondary extinction parameter. The secondary extinction parameter[11] refined to a value of $0.59\ (15) \times 10^{-6}$. The R index for reflections with $F_o^2 > 3\sigma(F_o^2)$ was 0.036. The final difference map showed maximum excursions of +0.25 and −0.22 e Å^{-3}.

Powder Second Harmonic Generation Measurements. Measurements of the powder SHG efficiencies were performed with the fundamental (1064 nm) of a Q-switched Nd:YAG laser (Quanta-Ray Model DCR-2A) or the first Stokes line (1907 nm) obtained by Raman shifting the Nd:YAG fundamental in H_2 gas. The appropriate excitation beam was selected and split into two beams, and each beam was long-pass filtered (using Schott RG-850 or RG-1000 filters) to remove stray radiation at the second harmonic frequency. The beams were attenuated and weakly focused so as to deliver 100–500 μJ in a spot size of 2–3-mm diameter to the specimens under study. The two beams were used to excite a sample of the material to be measured and a powdered urea sample, the signal from which was used to provide a reference signal for normalization of shot-to-shot laser pulse amplitude fluctuations. The SH signals from the sample and the urea reference were analyzed by separate optical and electronic systems.

The excitation beams were incident on the samples at an angle of ~65°. The diffusely backscattered SH radiation was collected by using a 2-in. f/1.5 lens situated between the normal to the sample and the specular reflected exciting beam. f/no. matched lenses (f/3.5 or f/4) focused the collected light onto the slits of monochromators (0.25 or 0.2 m with 6- or 10-nm band pass). Schott KG-3 filters (for 1064-nm excitation) or water filters (for 1907-nm excitation) were used before the monochromators to eliminate collected excitation radiation.

The SH signals were detected with photomultiplier tubes (Hamamatsu Models R928 or R406) whose outputs were amplified (×100 by using two Comlinear CLC-100 amplifiers, DC 500-MHz bandwidth) and fed into boxcar integrators (Stanford Research Inc., Model SR-250). Typically, integrator gate widths of 10 ns were used. The outputs of the integrators were digitized by an analog to digital convertor (Analog Devices RTI 802) interfaced to a microcomputer (IBM PC-AT), which computed the normalized SH signal. True SH signals were distinguished from possible artifacts (fluorescence, inelastically scattered light, etc.) by tuning the monochromator to verify that the signal was narrow band around the SH frequency and by observing the signal in real time on a wide-bandwidth oscilloscope to ensure that only a prompt signal that essentially followed the laser pulse profile was observed.

Samples were unsized microcrystalline powders obtained by gently grinding materials with a mortar and pestle. The broad distribution of particle sizes was estimated to span from about 40 to 150 μm. Roughly 50 mg of powder was placed between glass microscope slide cover slips, the material was spread out to ~0.5 mm powder layer thickness, and the edges were sealed. Given the uncharacterized particle sizes and the possibility of preferential orientation of particles in assembling the sample, the uncertainties in the measured efficiencies can be quite large, perhaps factors of 2 or more, and therefore should be taken as a qualitative measurement.

Results

The crystal structures reveal that all four molecules are approximately planar and fully extended (Figure 1). Even the unbridged molecule, *p*-amino-*p*′-nitrobiphenyl (I), which might be expected to be distorted from planarity because of steric repulsion between the ortho hydrogen atoms, shows a torsion angle about the phenyl–phenyl bond [C(14)–C(24)] of only 2.5 (5)°. The molecule is also slightly bent so that the dihedral angle between the planes of the two rings is 5.0 (2)°. There is no unusual libration of the molecule about its long axis, which might suggest disorder involving nonplanar moieties. Such a libration was observed in biphenyl, even at low temperature, and it has been suggested that at even lower temperatures biphenyl would undergo a phase transition to a nonplanar structure.[15] We see no reason to predict such a transition for compound I.

The bond lengths and angles are summarized in Table III. In general the three acetylene–bridged compounds, II–IV, show effectively the same dimensions for both the *p*-nitrophenyl and the *p*-aminophenyl groupings; that is, the differences between corresponding distances and angles in the three compounds are no longer than the differences between chemically equivalent (assuming C_2 symmetry) values *within* the individual molecules. However, both types of differences are often larger than the formal esd's should permit, by factors ranging up ~3.0; there appear to be small but significant distortions from C_2 symmetry in all three compounds (perhaps caused by those ubiquitous "packing forces"). Regardless, we have chosen to consider the equivalent distances to be averageable both within and between the three bridged compounds; the esd's of the average values (Table III) include the goodness-of-fit multiplier reflecting the scatter.

All four compounds feature the same arrangement of *inter*-molecular $NH_2\cdots NO_2$ hydrogen bonds, a zig-zag chain (Figure 2) directed along the short unit cell direction, and perpetuated into a two-dimensional sheet by a glide plane perpendicular to that direction. But the species of the arrangement change appreciably as bridging acetylene groups are added (see Figure 3). Whereas successive molecules along the chain are not far from parallel in compound I ($n = 0$), they are nearly perpendicular in compounds III and IV. As a result, one of the two hydrogen bonds

---

(13) Eastmond, R.; Walton, D. R. m. *Tetrahedron* **1972**, *28*, 4591–4599.

(14) The product, (*p*-nitrophenyl)butadiyne, is somewhat unstable at room temperature and was used immediately after synthesis. It was characterized by comparison of its' UV–vis absorption spectrum to that published previously (ref 13).

(15) Charbonneau, G. P.; Delugeard, Y. *Acta. Crystallogr., Sect. B* **1977**, *B33*, 1586–1588; **1976**, *B32*, 1420–1432.

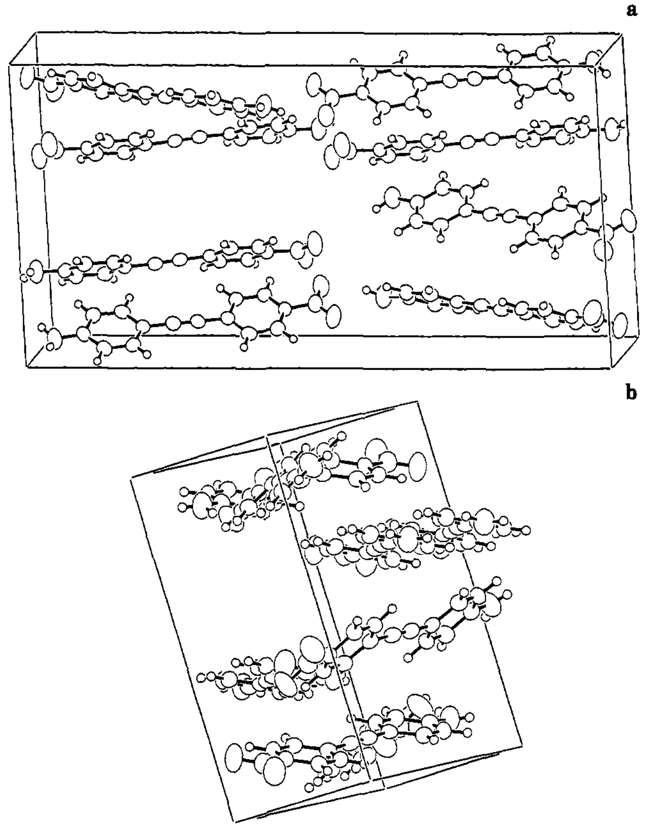

Figure 2. An ORTEP view of the contents of one unit cell (outlined) for molecule II (a) viewed perpendicular to the least-squares plane of all the atoms and (b) rotated by 90°. Thermal ellipsoids and hydrogen atoms as in Figure 1.

becomes grossly nonlinear in III and IV. The cogent distances and angles are given in Table IV. One notes that the N(2)···O(2) distance in this nonlinear bond remains nearly constant in going from I to IV, whereas the more linear N(2)···O(1) bond lengthens appreciably, from 3.02 to 3.34 Å. This apparent loss in hydrogen-bonding stability in the acetylene-bridged compounds is perhaps regained through more efficient packing elsewhere in the two-dimensional sheet, the aromatic rings fitting more compactly into the region around the acetylene groups.[16] It is also worth noting that there are no intermolecular interactions between the aromatic rings of molecules in the unit cell. In all of the compounds the aromatic rings of adjacent molecules lie at an angle large enough to preclude a "graphitic" (π–π) type of interaction (Figure 2b). The absence of this type of interaction may be due to the strong hydrogen bonding, which overcomes the relatively weak π–π interactions to dominate the crystal packing.

Structural Manifestations of Ground-State Charge-Transfer Character. Many aromatic donor–acceptor molecules, such as *p*-nitroaniline, possess a high degree of charge-transfer character in the ground state. This transfer of charge from donor to acceptor is conventionally thought of as occurring by bond migration through the conjugated framework, ultimately favoring a quinonoid resonance structure.[1]

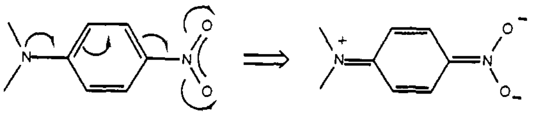

Structurally this manifests itself in specific distortion of the molecular framework reflecting the localized bonding pattern of the quinonoid resonance form. The amount of quinonoid character in the structure gives an indication of the degree to which the charge has migrated though the conjugated backbone. This resonance structure for the molecules discussed here is

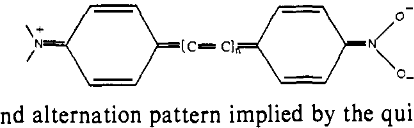

The bond alternation pattern implied by the quinonoid resonance structure is pronounced in *p*-nitroaniline.[1a] Both C–N bonds are short relative to aniline[17] [1.355 (2) vs 1.402 (2) Å] and nitrobenzene[18] [1.434 (2) vs 1.492 (2) Å], suggesting an appreciable degree of double-bond character. The benzene ring also shows decided bond alternation with a short C2(6)–C3(5) (ortho–meta) bond distance relative to the same bond in aniline and nitrobenzene [1.367 (2) v 1.394 (2) and 1.403 (2) Å, respectively]. Conversely, the remaining carbon–carbon bonds in the ring are elongated. As a further point of comparison, the structure of the hydrochloride salt of *p*-nitroaniline[19] in which the charge-transfer character has been eliminated shows equivalent bonds—within experimental error—[average 1.378 (6) Å] around the benzene ring as well as longer carbon–nitrogen distances [1.478 (5) Å for nitro and 1.472 (5) Å for the protonated amine].

For the acetylene-bridged compounds (II–IV) many of the distortions to the molecular framework are similar, though not as pronounced, as those in *p*-nitroaniline. For the aniline group

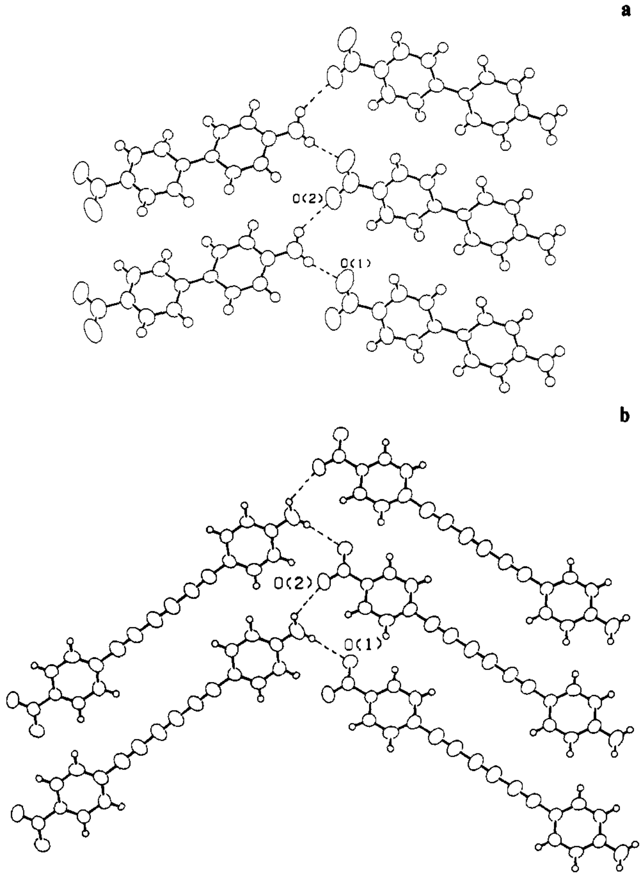

Figure 3. ORTEP drawing showing variations in the hydrogen-bonding network in going from compound 1 (a) to compound IV (b).

---

[16] It is worth noting that all of the structures show coplanarity of the phenyl rings despite wide variations in the crystal packing throughout the series. This might suggest a tendency toward planarity induced by *intra*molecular effects (charge-transfer character) that is largely insensitive to the *inter*molecular forces. However, as pointed out for compound I, separating the contribution from the *inter*- and *intra*molecular interactions is difficult.

(17) Lister, D. G.; Tyler, J. K.; Høg, J. H.; Larsen, N. W. *J. Mol. Struct.* **1974**, *23*, 253–264.

(18) Di Rienzo, F.; Domenicano, A.; Di Sanseverino, L. R. *Acta Crystallogr., Sect. B.* **1980**, *B36*, 586–591. These authors correctly point out that the original crystal structure of nitrobenzene (Trotter, J. *Acta Crystallogr.* **1959**, *12*, 884–888) possesses a high degree of uncertainty with large esd's for the bond distances and angles. For the purposes of comparison we have chosen to use the bond distances and angles of nitrobenzene, which were obtained from microwave spectroscopy and reported in Table 6 of this reference.

(19) Ploug-Sørensen, G.; Andersen, E. K. *Acta Crystallogr., Sect. B* **1982**, *B38*, 671–673.

Table III. Bond Distances (Å) and Angles (deg) for Compounds I–IV

	compound					
	II (n = 1)	III (n = 2)	IV (n = 3)	av	no.[a]	I[b] (n = 0)
			Distance			
N(1)–O(1)	1.224 (3)	1.224 (3)	1.226 (2)			
N(1)–O(2)	1.217 (3)	1.229 (3)	1.221 (2)	1.224 (2)	6	1.228 (6)
N(1)–C(11)	1.462 (3)	1.460 (4)	1.466 (2)	1.464 (2)	3	1.476 (9)
C(11)–C(12)	1.376 (3)	1.369 (4)	1.374 (2)			
C(11)–C(16)	1.378 (3)	1.384 (4)	1.384 (2)	1.378 (2)	6	1.366 (7)
C(12)–C(13)	1.376 (4)	1.369 (5)	1.378 (2)			
C(15)–C(16)	1.377 (4)	1.369 (5)	1.373 (2)	1.375 (2)	6	1.379 (7)
C(13)–C(14)	1.399 (3)	1.397 (5)	1.398 (2)			
C(14)–C(15)	1.398 (4)	1.381 (5)	1.386 (2)	1.393 (3)	6	1.389 (6)
C(14)–C(1)	1.435 (3)	1.437 (5)	1.431 (2)	1.433 (2)	3	
C(14)–C(24)						1.481 (8)
C(1)–C(2)		1.183 (5)	1.194 (2)			
C(2)–C(3)			1.369 (2)			
C(3)–C(8)			1.208 (2)			
C(8)–C(9)			1.368 (2)			
C(1)–C(10)	1.183 (4)					
C(2)–C(9)		1.388 (5)				
C(9)–C(10)		1.203 (5)	1.203 (2)			
C(10)–C(24)	1.436 (3)	1.422 (4)	1.425 (2)	1.426 (3)	3	
C(23)–C(24)	1.398 (3)	1.385 (4)	1.388 (2)			
C(24)–C(25)	1.394 (3)	1.402 (4)	1.407 (2)	1.397 (4)	6	1.395 (6)
C(22)–C(23)	1.370 (4)	1.369 (5)	1.365 (2)			
C(25)–C(26)	1.372 (4)	1.374 (5)	1.368 (2)	1.368 (2)	6	1.382 (7)
C(21)–C(22)	1.391 (4)	1.383 (5)	1.395 (2)			
C(21)–C(26)	1.391 (4)	1.384 (5)	1.390 (2)	1.391 (2)	6	1.387 (6)
N(2)–C(21)	1.379 (4)	1.384 (5)	1.381 (3)	1.381 (2)	3	1.368 (9)
			Angle			
O(2)–N(1)–O(1)	122.8 (2)	122.3 (3)	122.9 (1)	122.8 (1)	3	124.6 (7)
C(1)–N(1)–O(1)	118.8 (2)	118.7 (2)	118.6 (1)			
C(1)–N(1)–O(2)	118.4 (2)	118.9 (2)	118.6 (1)	118.6 (1)	6	117.7 (4)
N(1)–C(11)–C(12)	118.4 (2)	120.1 (3)	119.3 (1)			
N(1)–C(11)–C(16)	119.2 (2	118.0 (3)	118.3 (1)	118.8 (3)	6	119.1 (4)
C(12)–C(11)–C(16)	122.4 (2)	121.9 (3)	122.3 (1)	122.3 (1)	3	121.8 (6)
C(11)–C(12)–C(13)	119.1 (2)	119.4 (3)	118.5 (1)			
C(11)–C(16)–C(15)	118.4 (2)	118.2 (3)	118.4 (2)	118.6 (2)	6	118.7 (5)
C(12)–C(13)–C(14)	120.2 (2)	120.1 (3)	120.7 (2)			
C(16)–C(15)–C(14)	120.8 (2)	121.3 (3)	121.1 (2)	120.7 (2)	6	121.9 (5)
C(13)–C(14)–C(15)	119.1 (2)	119.1 (2)	118.9 (2)	119.0 (1)	3	117.0 (6)
C(1)–C(14)–C(13)	119.7 (2)	121.3 (3)	120.9 (1)			
C(1)–C(14)–C(15)	121.2 (2)	119.6 (3)	120.2 (2)	120.5 (3)	6	
C(24)–C(14)–C(13)						121.5 (4)
C(14)–C(1)–C(2)		177.4 (4)	178.9 (2)			
C(14)–C(1)–C(10)	177.8 (3)					
C(1)–C(2)–C(9)		179.7 (4)				
C(1)–C(2)–C(3)			179.7 (2)			
C(2)–C(3)–C(8)			179.3 (2)			
C(3)–C(8)–C(9)			179.5 (2)			
C(8)–C(9)–C(10)			179.8 (2)			
C(2)–C(9)–C(10)		179.1 (4)				
C(1)–C(10)–C(24)	176.9 (3)					
C(9)–C(10)–C(24)		177.1 (3)	178.5 (2)			
C(14)–C(24)–C(23)						122.3 (4)
C(10)–C(24)–C(23)	120.9 (2)	120.7 (3)	120.7 (1)			
C(10)–C(24)–C(25)	121.6 (2)	121.4 (3)	121.6 (1)	121.1 (2)	6	
C(23)–C(24)–C(25)	117.6 (2)	117.8 (3)	117.7 (1)	117.7 (1)	3	115.4 (6)
C(22)–C(23)–C(24)	121.5 (2)	121.3 (3)	121.9 (2)			
C(26)–C(25)–C(24)	121.1 (2)	120.3 (3)	120.5 (1)	121.2 (3)	6	122.6 (4)
C(21)–C(22)–C(23)	120.5 (2)	121.2 (3)	120.3 (1)			
C(21)–C(26)–C(25)	120.8 (2)	121.4 (3)	121.1 (1)	120.8 (2)	6	120.8 (5)
C(22)–C(21)–C(26)	118.5 (2)	118.0 (3)	118.5 (1)	118.4 (1)	3	117.7 (6)
N(2)–C(21)–C(22)	120.6 (2)	119.8 (3)	120.2 (2)			
N(2)–C(21)–C(26)	120.9 (2)	122.1 (3)	121.3 (2)	120.8 (3)	6	121.2 (4)

[a] Number of values in average. [b] Average of either one or two values for compound I.

the carbon–nitrogen distance of the amine [C(21)–N(2)] is 1.381 (2) Å, which is shorter than aniline by 0.021 (3) Å but larger by 0.026 (3) Å than the same bond in *p*-nitroaniline. The bond distortions in the aniline ring are also quite similar to those of *p*-nitroaniline. The C(22)–C(23) bond length of 1.368 (2) Å is the same as *p*-nitroaniline, as is the concomitant lengthening of the adjacent carbon–carbon bonds. Furthermore, the interior bond angle at the amine carbon [C(26)–C(21)–C(22)] is virtually identical with that of *p*-nitroaniline [118.4 (1)°], as are the angles centered at C(26) and C(22). The angle at the bridgehead carbon, C(25)–C(24)–C(23), is smaller by 1.5° than the same angle in diphenylacetylene. Taken together these are suggestive of a degree of quinonoid character in the aniline functional group. The pattern is not nearly as pronounced for the nitrobenzene group. The carbon–nitrogen [C(11)–N(1)] distance is shorter than that of nitrobenzene [1.464 (2) vs 1.492 (2) Å] but longer than that of

Table IV. Hydrogen-Bonding Distances and Angles

	compound			
	I	II	III	IV
	Distance			
N(2)–H($N2_a$)	0.94 (5)	0.95 (3)	0.91 (4)	0.84 (3)
N(2)···O(1)	3.025 (6)	3.156 (3)	3.381 (4)	3.340 (3)
H($N2_a$)···O(1)	2.10 (5)	2.23 (3)	2.48 (4)	2.51 (3)
N(2)–H($N2_b$)	0.93 (5)	0.81 (3)	0.87 (4)	0.92 (3)
N(2)···O(2)	3.130 (6)	3.143 (3)	3.182 (4)	3.150 (3)
H(N2b)···O(2)	2.34 (5)	2.47 (3)	2.64 (4)	2.48 (3)
	Angle			
N(2)–H($N2_a$)···O(1)	168	165	175	173
N(2)–H(N2b)···O(2)	143	142	121	130

p-nitroaniline. The phenyl group shows some bond alternation with the C(12)–C(13) bond distance [1.375 (2) Å] falling between that of nitrobenzene [1.403 (2) Å] and that of *p*-nitroaniline [1.367 (2) Å]. It is significant, however, that this bond distance and the angle centered at the bridgehead carbon, C(13)–C(14)–C(15), are identical (within error) with those of diphenylacetylene.[21] The interior bond angle at the nitro carbon, C(12)–C(11)–C(16), [122.3 (1)°] is larger than in *p*-nitroaniline [120.0 (2)°] and smaller than in nitrobenzene [125 (1) °], but the C(11)–C(12) bond distance [1.378 (2) Å] is the same (within error) as that in nitrobenzene [1.375 (1) Å]. It is clear that the charge-transfer-induced distortions in the nitrophenyl group are localized primarily around the nitro to phenyl bond with only minor distortions to the rest of the ring. A comparison of the relevant bond distances between II, *p*-nitroaniline, nitrobenzene, and aniline follows.

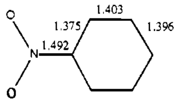

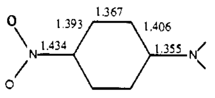

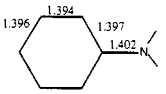

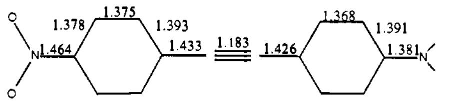

In general, based on the structural parameters for the aniline and nitrobenzene groups, compounds II–IV show distortions of the molecular framework toward a quinonoid resonance form. While these distortions are less pronounced than in *p*-nitroaniline, they do imply a fair degree of charge-transfer character in the ground state. As previously stated, the bond distances (and hence the quinonoid pattern of distortions) in the aniline and nitrobenzene groups of II–IV are virtually invariant throughout the series, suggesting that the communication between the donor and acceptor remains relatively constant as the molecular get longer. This is consistent with our previous spectroscopic observation that the energy and intensity of the ICT band remained unchanged throughout the series of molecules.[6]

One structural feature that is inconsistent with the general idea of a fully quinonoid distortion of the molecular framework is the acetylene linkers themselves. If the resonance form drawn above were strictly correct, the acetylene linker would be expected to move from an alternating single-bond–triple-bond pattern to a more cumulene-type structure with a decrease in the single-bond lengths and a concomitant increase in the triple-bond lengths. The opposite is true for *p*-amino-*p*′-nitrodiphenylacetylene (II) where the triple bond length [1.183 (4) Å, C(1)–C(10)] is shorter than in diphenylacetylene [1.198 (4) Å][20] and considerably shorter than in acetylene itself (1.203 Å).[21] The single bonds to acetylene show no unusual distortions and are the same as in diphenylacetylene [1.433 (2) vs 1.438 (3) Å]. As the number of acetylenes increases the lengths of the triple bonds also increase and approach that of acetylene itself (ca. 1.20 Å), with the triple bond closest to the nitrophenyl group being always somewhat shorter. The acetylene linkers show a pronounced single-bond–triple-bond pattern possessing no cumulene character.

If the transfer of charge from donor to acceptor were a fully delocalized phenomenon, then some degree of quinonoid character would be expected. The fact is that while the quinonoid type of stucture is evident in the aniline group and, to a much lesser extent, in the nitrobenzene group, it is totally absent from the conjugated linker. This suggests a somewhat modified view of charge transfer through a conjugated system. The acetylene linker acts as a conduit to transfer charge into what are ultimately highly localized orbitals. The negative charge resides in a vacant π^* orbital on the nitro group and the positive charge is nominally on the amine. The positive charge on the amine withdraws electron density from the π system on the ring, thus distorting the aniline group toward the observed quinonoid form. The negative charge in the nitro π^* orbital results in back-donation into the ring, shortening the carbon–nitrogen bond. Apparently the energy required to structurally rearrange the molecules into a fully quinonoid form is greater than the energy obtained from delocalization of the charge. For the bridging acetylenes in particular the formation of two new π bonds from a triple bond and two single bonds (with the concomitant changes in bond length) is energetically unfavorable and not compensated for by gains in resonance energy. The key point is that the charge transfer is characterized by very localized effects with charges residing predominantly on the amino and nitro functional groups themselves and distorting the molecular framework over only a few adjacent bonds.

It might be reasonable to assume that the localized structural changes occur *not* as the result of *intra*molecular charge-transfer character but through *inter*molecular interactions. It is clear from the strong hydrogen bonding observed in the crystal structures that this type of interaction is not insignificant. This would suggest that the transfer of charge occurs not through the acetylene bridge but from direct amine to nitro interactions between adjacent molecules. However, evidence for the participation of the acetylene bridge is clear from a consideration of the structure of *p*-(*N*,*N*-dimethylamino)-*p*′-nitrodiphenylacetylene, which was determined by Stamatoff and co-workers.[22] This molecule shows a bonding pattern identical with that observed in the nonmethylated molecules, with the nitrophenyl and aniline groups showing an even more pronounced bond alternation.[23] No evidence of quinonoid character is observed over the extent of the bridge, with the linking acetylene having a short carbon–carbon triple-bond distance [1.197 (5) Å]. The essential point here is that the presence of the methyl groups prevents *inter*molecular interactions of the type observed in the unmethylated series. No hydrogen bonding is observed with the closest through-space amine nitrogen to oxygen distance for the methylated compound being 3.397 (5) Å. This is in contrast to amine nitrogen to oxygen distances of 3.150 (3) Å or less (Table IV), directed through strong hydrogen bonds, in the unmethylated series of molecules. It is evident from these data that the charge-transfer character of the ground state is an *intra*molecular phenomenon that requires transfer of charge through the acetylene linker. In short, the acetylenic linking groups allow communication between the donor and acceptor groups without themselves being electronically altered.

The structure of *p*-amino-*p*′-nitrobiphenyl (I) shows a number of features that differ from the acetylene-bridged compounds. The phenyl groups show little bond localization in comparison to the bridged compounds [C(22)–C(23) and C(25)–C(26) are 1.382 (7) Å in I and 1.368 (2) Å for the bridged compounds]. In fact, all of the carbon–carbon bonds in the aniline group are, within experimental error, of equal length and only somewhat shorter than in aniline itself. The carbon–nitrogen bond to amine [C(21)–N(2)] is quite short and is close to that observed for *p*-

---

(20) Mavridis, A.; Moustakali-Mavridis, I. *Acta. Crystallogr. Sect. B* **1977**, *B33*, 3612–3615.

(21) Lafferty, W. J.; Thibault, R. J. *J. Mol. Spectrosc.* **1964**, *14*, 79–96.

(22) (a) Buckley, A.; Choe, E.; DeMartino, R.; Leslie, T.; Nelson, G.; Stamatoff, J.; Stuetz, D.; Yoon, H. *Polym. Prepr., PMSE* **1986**, *54*, 502–509. (b) Stamatoff, J., private communication.

(23) This is probably due to the stronger donating ability of the alkylated amine; alternatively, the strong hydrogen bonding in the structure of the nonalkylated compounds may decouple the donor and acceptor groups.

Table V. Second Harmonic Generation Data for Compounds I–IV

compd	SHG intensity vs urea	
	1907 nm	1064 nm
I	2.5	3.0
II	0.4	0.04–0.2
III	0.1	0.02
IV	0.7	0.03

nitroaniline [1.368 (9) vs 1.355 (2) Å]. For the nitrobenzene group the carbon–nitrogen bond [C(11)–N(1)] is 1.476 (9) Å, which is only somewhat shorter than that of nitrobenzene; however, as with the acetylene-bridged compounds, bond alternation in the nitrophenyl ring is somewhat more pronounced than in nitrobenzene itself. Another difference between I and the bridged compounds lies in the angles involving the bridgehead atoms C(14) and C(24). The interior angles C(13)–C(14)–C(15) and C(23)–C(24)–C(25) are smaller by ~2° in compound I, and the neighboring angles at C(13), C(15), C(23), and C(25) are larger by ~1°—effects that are most likely due to repulsion between the ortho hydrogens. In general, the structural features of *p*-amino-*p'*-nitrobiphenyl indicate a lower degree of ground-state charge-transfer character than is observed in the bridged compounds. That the communication between the donor and acceptor is somewhat less than in the acetylene-linked compounds is supported spectroscopically by the ICT band, which, for *p*-amino-*p'*-nitrobiphenyl, lies to higher energy by ~50 cm^{-1} than for the acetylene-bridged compounds.

While it might be argued that the observed planarity of the molecule [torsion angle 2.3 (5)°] is induced by charge-transfer character in the ground state, separating this effect from the intermolecular ones is difficult.[16] Biphenyl itself is essentially planar in the solid state (with a libration about the long axis)[15] but shows a twist angle of 40–45° in the gas phase.[24] Calculations by Casalone and co-workers suggest that the twisted configuration is the preferred geometry for the isolated molecule and that the planar structure adopted in the crystal is enforced by *inter*molecular interactions.[25] Recent experimental work has shown that in fact the barrier to rotation around the phenyl–phenyl bond is quite small (~150 cm^{-1}).[26] Other para-substituted biphenyls (dinitro,[27] nitro,[28] and dimethyl[29]) are twisted in the crystal with torsional angles between 30 and 40°, while *p*-dihydroxybiphenyl is planar.[30] In general, the adoption of a twisted or planar structure in the solid state seems to fit no specific pattern and is dictated by a variety of subtle effects.

Powder Second Harmonic Generation. The molecules reported here were synthesized in the course of our study of the nonlinear optical properties of new organic materials. They possess a combination of structural and electronic features (ICT transitions and donor–acceptor groups separated by a conjugated framework) that has been shown to give rise to large second-order hyperpolarizabilities (β). The second-order hyperpolarizabilties are microscopic molecular properties that can give rise to the macroscopic second-order susceptibilities [$\chi^{(2)}$]. A manifestation of the second-order susceptibility is second harmonic generation (SHG) or frequency doubling. We measured the SHG efficiencies for this series of donor–acceptor diphenylacetylenes.[31] Powder SHG efficiencies were determined, relative to urea, by a modification of the Kurtz powder technique.[32] A tabulation of second harmonic intensity data for this series of molecules is reported in Table V. While it is necessary for the molecules comprising a material to have a large β in order for the material to exhibit a substantial $\chi^{(2)}$, this is not sufficient in and of itself. The second-order susceptibility, [$\chi^{(2)}$], is a third rank tensorial quantity, which is nonvanishing only for noncentrosymmetric space groups. In short, for a material to produce frequency doubling the molecules must pack in a noncentrosymmetric space group.[5,22a]

The only molecule in the series that crystallizes in a noncentrosymmetric space group ($Pca2_1$) is *p*-amino-*p'*-nitrobiphenyl (I), which, predictably, has the largest SHG signal at 2.5 times urea (determined at 1907 nm) in agreement with previous measurements.[33] It is interesting to note that while the other molecules in the series all crystallize in centrosymmetric space groups the measured SHG signals are not rigorously zero, as theory would predict, but as much as 0.7 times urea for IV. The values for molecules II–IV are smaller for 1064-nm compared to 1907-nm excitation. This is likely due to increased absorption of the second harmonic at the shorter wavelength. It has been proposed[34] that the origin of the SHG signal in *single* centrosymmetric crystals might be from defect sites in the crystal or from the surface where the crystal symmetry is broken. In *powder* SHG experiments, where the sample under study is comprised of a large number of microcrystals, an additional source of SHG activity can come from polymorphism. For materials prone to polymorphism, noncentrosymmetric crystals (an SHG active phase) may form along with centrosymmetric crystals in the bulk microcrystalline powder. For molecules possessing a high β, a small amount of an SHG active phase could give rise to a finite signal in a material that is nominally centrosymmetric.[35] This is a point that should be kept in mind if the powder SHG measurements are used as a tool for assigning noncentrosymmetric space groups.[36]

Summary. Several interesting observations concerning the nature of ground-state charge transfer have emerged from the structral analysis of this series of molecules. The pronounced bond alternation in the nitrophenyl acceptor and the aminophenyl donor groups shows clearly that the ground state possesses a high degree of charge-transfer character. What is structurally unusual is the total absence of such character in the bridging acetylenes; in fact they possess a pronounced single-bond–triplet-bond alternation pattern with none of the "quinonoid" resonance structure that might be expected from the migration of charge through a totally conjugated framework. It is apparent that the conjugated acetylene linkers are necessary to transfer charge, but are not structurally altered in the process that leads to the conclusion that, once transferred, the charges are highly localized. Furthermore, the degree of charge-transfer character appears to be invariant throughout the series, an observation that compares with our earlier report on the invariance of the ICT band with acetylene length for this series. It is evident that in both the ground state and the excited state the interactions between the donor and the acceptor are very strong but also are relatively independent of the conjugated linker.

Acknowledgment. We thank Dr. J. B. Stamatoff of Hoechst Celanese for providing details of the crystal structure of *p*-(*N*,*N*-dimethylamino)-*p'*-nitrodiphenylacetylene. The research reported in this paper was performed by the Jet Propulsion Laboratory, California Institute of Technology, as part of its Center for Space Microelectronics Technology, which is sponsored by the Strategic Defense Initiative Organization/Innovative Science and Technology Office through an agreement with the National Aeronautics and Space Administration (NASA).

---

(24) Bastiasen, O. *Acta. Chem. Scand.* **1949**, *3*, 408.

(25) Casalone, G.; Mariani, C.; Mugnoli, A.; Simonetta, M. *Mol. Phys.* **1968**, *15*, 339–348.

(26) Im, H.-S.; Bernstein, E. R. *J. Chem. Phys.* **1988**, *88*, 7337–7347.

(27) Boonstra, E. G. *Acta Crystallogr.* **1963**, *16*, 816–823.

(28) Casalone, G.; Gavezzotti, A.; Simonetta, M. *J. Chem. Soc., Perkin Trans.* **1973**, 342-345.

(29) Casalone, G.; Mariana, C., Mugnoli, A.; Simonetta, M. *Acta Crystallogr.* **1969**, *B25*, 1741–1750.

(30) Farag, M. S.; Kader, N. A. *J. Chem. U.A.R.* **1960**, *3*, 1.

(31) Perry, J. W.; Stiegman, A. E.; Marder, S. R.; Coulter, D. R.; Beratan, D. N.; Brinza, D. E.; Klavetter, F. L.; Grubbs, R. H. *Proc. SPIE—Int. Soc. Opt. Eng.* **1988**, *971*, 17.

(32) Kurtz, S. K.; Perry, T. T. *J. Appl. Phys.* **1968**, *39*, 3798.

(33) Davydov, B. L.; Kotovshchikov, S. G.; Nefedov, V. A. *Sov. J. Quantum Electron.* (*Engl Transl.*) **1977**, 7(1), 129.

(34) Dick, B.; Hockstrasser, R. M.; Trommsdorf, H. P. In *Nonlinear Optical Properties of Organic Molecules and Crystals*; Chemla, D. S., Zyss, J., Eds.; Academic Press: New York 1987; Vol. II, 159.

(35) (a) Tam and co-workers observed variations in the SHG intensity for the molecules *p*-bromo-*p'*-nitrodiphenylacetylene as a function of recrystallization solvents. This behavior can also be attributed to the effects of polymorphism. Tam, W., personal communication. (b) Tabei, H.; Kurihara, T.; Kaino, T. *Appl. Phys. Lett.* **1987**, *50*, 1855.

(36) Dougherty, J. P.; Kurtz, S. K. *J. Appl. Crystallogr.* **1976**, *9*, 145.

J. Am. Chem. Soc. **1989**, *111*, 8779–8784

Note Added in Proof. While the series of substituted diphenylacetylenes reported in this paper exhibit centrosymmetric crystal phases (from acetonitrile solution) and are essentially SHG inactive, we[31] and others[35] have recently shown that highly SHG active (efficiencies up to 200 times urea) derivatives, e.g., NH_2, CO_2CH_3, CH_3S, and NO_2, of diphenylacetylenes can be prepared.

Registry No. I, 1211-40-1; II, 7431-22-3; III, 110175-15-0; IV, 110175-16-1; $Cu(C{\equiv}CC_6H_4\text{-}p\text{-}NO_2)$, 123207-77-2; *p*-iodoaniline, 540-37-4; (*p*-nitrophenyl)acetylene, 937-31-5; (*p*-aminophenyl)acetylene, 14235-81-5; (triethylsilyl)acetylene, 1777-03-3, 7642-33-3.

Supplementary Material Available: Tables of anisotropic displacement factors (4 pages); observed and calculated structure factors (35 pages). Ordering information is given on any current masthead page.

Characterization of (Methylcyclopentadienyl)trimethylplatinum and Low-Temperature Organometallic Chemical Vapor Deposition of Platinum Metal

Ziling Xue,[†] M. Jane Strouse,[†] David K. Shuh,[†] Carolyn B. Knobler,[†] Herbert D. Kaesz,[*,†] Robert F. Hicks,[‡] and R. Stanley Williams[†]

Contribution from the Department of Chemistry and Biochemistry, University of California, Los Angeles, California 90024-1569, and Department of Chemical Engineering, University of California, Los Angeles, California 90024-1592.

Received March 6, 1989

Abstract: (η^5-Methylcyclopentadienyl)trimethylplatinum, (η^5-MeCp)$PtMe_3$, **1** (MeCp = $CH_3C_5H_4$), is synthesized from trimethylplatinum iodide and sodium methylcyclopentadienide by the method of Fritz and Schwarzhans. By using some care in the purification of bis(methylcyclopentadiene) from dicyclopentadiene, a sample of **1** is obtained showing a melting point of 29.5–30.0 °C and a vapor pressure of 0.053 Torr at 23 °C. ^1H and ^{13}C NMR spectra have been obtained, the latter both in solution as well as in the solid state. Coupling constants to the cyclopentadienyl ring carbons are found to differ, Hz: $^{195}Pt-^{13}C_{Me} = 13.62$, while $^{195}Pt-^{13}C_H = 2.82$ or 5.34. Five separate resonances are observed for the ring carbon atoms of the MeCp group in the solid state $\{^1H\}^{13}C$ NMR. However, only one signal is observed at −73 °C or higher for the three methyl groups on Pt, indicating a low barrier for rotation of these groups in the solid state. The structure has been determined on a single crystal of **1** at −143 °C: monoclinic, space group $P2_1$, with $a = 7.159$ (2) Å, $b = 11.092$ (3) Å, $c = 6.004$ (1) Å, and $\beta = 106.806$ (6)°. The structure was solved and refined by using 907 observed ($I > 3\sigma(I)$) independent reflections measured on a Picker automated diffractometer. Refinement uncorrected for absorption converged at $R = 0.034$ and $R_w = 0.060$. The principal finding, of significance to the solid-state NMR, is the intermolecular contacts of 3.98, 4.55, and 4.94 Å between closest ring-carbon atoms on independent molecules in adjacent unit cells. These contacts are too close to permit rotation of the MeCp rings. The ring is pentahapto-bonded with almost identical Pt to ring-carbon distances within the limited accuracy of this determination, Å: $C_{(Me)}-Pt = 2.266$, $C_{(H)}-Pt = 2.260$, 2.314, 2.354, and 2.324. For deposition of metallic platinum, a stream of Ar gas at ambient pressure is first saturated with the vapor of **1** at 23 °C. This is then conducted into a chamber containing H_2 gas such that the ratio of saturated Ar:H_2 = 4:1. A substrate such as a glass slide or a Si(100) wafer, placed near the outlet of the saturated Ar gas stream and heated to 120 °C, becomes coated with a film of highly reflective Pt metal. The films have been characterized by powder X-ray diffraction (indicating a crystalline nature) and with X-ray photoelectron spectroscopy (XPS). A high purity, i.e., less than 1 atom % C, is indicated.

Thin films of platinum are used extensively in microelectronics device processing[1,2] and electrodeless metal plating.[3] Thermal deposition of platinum from the vapor phase has been reported with use of $Pt(acetylacetonate)_2$, $Pt(PF_3)_4$, or $Pt(CO)_2Cl_2$.[4–6] These depositions require high temperature (200–600 °C), and the films are contaminated by heteroatoms from the ligands. We have been interested in finding other volatile organometallic compounds to obtain platinum films of higher purity. The ready decomposition of tris(ethylene)platinum was already known.[7] However, this hydrocarbon precursor is much too unstable for long-range storage and handling. Recently our group[8] and others[9] have reported organometallic chemical vapor deposition (OMCVD) from hydrocarbon precursors. In our work,[8] platinum films of high purity (>99 atom %) and high crystal quality were obtained at 180 °C from $CpPtMe_3$ (Cp = cyclopentadienyl) in the presence of H_2. The need to have a liquid organometallic precursor for better control of evaporation has led us to investigate (methylcyclopentadienyl)trimethylplatinum, (MeCp)$PtMe_3$, reported[10] to be an oily substance at room temperature. Here we report our studies on this complex. A preliminary account of a part of this work has appeared.[11]

Experimental Section and Results

Preparation of (MeCp)$PtMe_3$, 1. Commercially available bis(methylcyclopentadiene) (Aldrich) is only 95% pure. The dimer is thermally

---

[†] Department of Chemistry and Biochemistry.

[‡] Department of Chemical Engineering.

(1) Green, M. L.; Levy, R. A. *J. Metals* **1985**, *37*, 63–71.

(2) Ghate, P. B. In *Thin Films and Interfaces*; Materials Research Society Symposium Proceedings, Ho, P. S., Tu, K. N., Eds.; Elsevier: New York, 1982; Vol. 10, pp 371–395.

(3) Bindra, P.; Roldan, J. *J. Electrochem. Soc.* **1985**, *132*, 2581–2589.

(4) Rand, M. J. *J. Electrochem. Soc.* **1973**, *120*, 686–693.

(5) Rand, M. J. *J. Electrochem. Soc.* **1975**, *122*, 811–815.

(6) Morabito, J. M.; Rand, M. J. *Thin Solid Films* **1974**, *22*, 293–303.

(7) Green, M.; Howard, J. A. K.; Spencer, J. L.; Stone, F. G. A. *J. Chem. Soc., Dalton Trans.* **1977**, 271–277.

(8) Chen, Y.-J.; Kaesz, H. D.; Thridandam, H.; Hicks, R. F. *Appl. Phys. Lett.* **1988**, *53*, 1591–1592.

(9) Gozum, J. E.; Pollina, D. M.; Jensen, J. A.; Girolami, G. S. *J. Am. Chem. Soc.* **1988**, *110*, 2688–2689.

(10) Fritz, H. P.; Schwarzhans, K.-E. *J. Organomet. Chem.* **1966**, *5*, 181–184.

(11) Kaesz, H. D.; Williams, R. S.; Hicks, R. F.; Chen, Y.-J.; Xue, Z.; Xu, D.; Shuh, D. K.; Thridandam, H. In *Chemical Perspectives of Microelectronic Materials*; Materials Research Society Symposium Proceedings, Gross, M. E., Jasinski, J. M., Yates, Jr., J. T., Eds.; Materials Research Society: Pittsburgh, PA, 1989; Vol. 131, pp 395–400.